JOURNAL OF AIRCRAFT
Vol. 40, No. 3, May–June 2003

Theoretical Solutions for Finite-Span Wings of Arbitrary Shapes Using Velocity Singularities

D. Mateescu,* J. F. Seytre,† and A. M. Berhe†
McGill University, Montreal, Quebec H3A 2K6, Canada

This paper presents a new method of solution for the finite-span wings of arbitrary shapes, which avoids the difficulties of the previous methods. This method uses velocity singularities in the Trefftz plane to derive the contributions in the solution of the circulation distribution caused by the changes in the spanwise variation of the wing chord and incidence. The new functions derived for these contributions contain both natural and forced symmetry and antisymmetry terms (which are absent in the previous methods) and thus represent a correct mathematical modeling of the physical problems that lead to highly accurate theoretical solutions. The method has been validated by comparison with the solutions obtained by Rasmussen and Smith and Carafoli for rectangular and tapered wings of uniform incidence, and with the panel method results by Katz and Plotkin. Accurate and efficient theoretical solutions of aeronautical interest are then obtained for wings with asymmetric incidence distributions caused by symmetric and antisymmetric deflections of flaps and ailerons and for wings with curved leading and trailing edges and variable incidence, which are difficult to model in current panel methods.

Nomenclature

b = wing semispan
bx, by, bz = dimensional Cartesian coordinates, with by axis along the wing span and bx axis parallel to the freestream velocity U_∞
$bc(y)$ = dimensional local wing chord
$c(y)$ = nondimensional local wing chord, $c_R = c(0)$, $c_T = c(1)$
c_a = nondimensional mean (average) wing chord, $\frac{1}{2}\int_{-1}^{1} c(y)\,\mathrm{d}y$
$\bar{c}(y)$ = $c(y)/c_a$
C_{Di} = induced drag coefficient, $2K\alpha_a^2\delta^*$
C_{Di} = $\lambda\alpha_a^2\int_{-1}^{1}\frac{1}{2}\bar{w}^*(y)\bar{\Gamma}_L(y)\,\mathrm{d}y$
C_L = lift coefficient, $2K(\alpha_a-\alpha_{ia}) = 2K_\lambda\alpha_a$
C_L = $\lambda\alpha_a\int_{-1}^{1}\bar{\Gamma}_L(y)\,\mathrm{d}y$
$C_l(y)$ = local lift coefficient, $4\alpha_a\bar{\Gamma}(y)/c(y)$
$C(s)$ = $(2/\pi)\cos^{-1}[(1+s)/2]^{\frac{1}{2}}$
$G(s, y)$ = $(2/\pi)\cosh^{-1}\{(1-y)(1+s)/[2(s-y)]\}^{\frac{1}{2}}$ for $y\in(-1, s)$, $(2/\pi)\sinh^{-1}\{(1-y)(1+s)/[2(y-s)]\}^{\frac{1}{2}}$ for $y\in(s, 1)$, and 0 for $y<-1$ or $y>1$
$\tilde{G}(s, X)$ = singular contribution in $\bar{\Gamma}(X)$ of a ridge situated at $X=s$, $(2/\pi)\cosh^{-1}\{(1-X)(1+s)/[2(s-X)]\}^{\frac{1}{2}}$
$G_0(y)$ = $G(0, y) = (2/\pi)\cosh^{-1}[(1+|y|)/2|y|]^{\frac{1}{2}}$
$g_{i,k}$ = $2\ell_{i+k}/(i+1)$
$H(s, y)$ = $\begin{cases}1 & \text{for } s<y<1\\ 0 & \text{for } y<s \text{ or } y>1\end{cases}$
$H(s, -y)$ = $\begin{cases}1 & \text{for } -1<y<-s\\ 0 & \text{for } y<-1 \text{ or } y>-s\end{cases}$
I_j = $J_j(0)$, recurrence formula: $I_j = [(j-1)/j]I_{j-2}$, with $I_0=1$ and $I_1=2/\pi$
$J_j(s)$ = $[(j-1)/j]J_{j-2}(s) + (2/\pi j)s^{j-1}[1-s^2]^{\frac{1}{2}}$, with $J_0(s) = 2C(s)$ and $J_1(s) = (2/\pi)[1-s^2]^{\frac{1}{2}}$
ℓ_k = $[1+(-1)^k]/2$
q = wing taper ratio, $1-c_T/c_R$
$s, -s$ = spanwise coordinates of ridges (where wing boundary conditions change)
$s_1, -s_2$
U_∞ = freestream velocity
$v(y, z)$, $w(y, z)$ = perturbation velocity components along y and z-axes on the wing ($x=0$)
$v^*(y, z)$, $w^*(y, z)$ = perturbation velocity components in the Trefftz plane ($x\to\infty$); $w^*(y, z) = 2w(y, z)$
$\bar{w}^*(y)$ = nondimensional velocity component in Trefftz plane ($x\to\infty$), $w^*(y, 0)/(\alpha_a U_\infty)$
X = complex variable in the Trefftz plane ($x\to\infty$), $y+iz$
x, y, z = nondimensional Cartesian coordinates ($x = bx/b$, $y = by/b$, $z = bz/b$)
α_a = mean (average) wing incidence, $\frac{1}{2c_a}\int_{-1}^{1} c(y)\alpha(y)\,\mathrm{d}y$
α_{ia} = mean (average) induced incidence, $\alpha_a\alpha_{ia}^*$, where $\alpha_{ia}^* = \frac{1}{2}\int_{-1}^{1}\bar{c}(y)\frac{1}{2}\bar{w}^*(y)\,\mathrm{d}y$
α_{ia} = $(C_L/\pi\lambda)(1+\tau)$
$\alpha(y)$ = local wing incidence, $\alpha_R = \alpha(0)$, $\alpha_T = \alpha(1)$
$\bar{\alpha}(y)$ = $\alpha(y)/\alpha_a$
$\bar{\Gamma}_L(y)$ = nondimensional circulation around a local wing section
$\Gamma(y)$ = spanwise distribution of the circulation
$\bar{\Gamma}(y)$ = nondimensional circulation, $\Gamma(y)/[2b\alpha_a U_\infty]$
$\gamma(y)$ = distributed circulation on the wing, $\mathrm{d}\Gamma(y)/(b\,\mathrm{d}y)$
δ = induced drag factor, $(\pi\lambda/2K)[\delta^*/(1-\alpha_{ia}^{*2})^2]-1$

Received 31 March 2002; revision received 9 December 2002; accepted for publication 10 December 2002.

*Professor, Aeronautical Program, Aerospace Program Director, Department of Mechanical Engineering. Associate Fellow AIAA.
†Graduate Student, Department of Mechanical Engineering.

$$\delta^* = \frac{1}{2}\int_{-1}^{1} \bar{c}(y)\frac{1}{2}\bar{w}^*(y)\left[\bar{\alpha}(y) - \frac{1}{2}\bar{w}^*(y)\right] dy$$

λ = wing aspect ratio, $4b^2/S = 2/c_a$, where $S = 2b^2c_a$ is the wing area
τ = lift coefficient factor, $(\pi\lambda/2K)[\alpha^*_{ia}/(1-\alpha^*_{ia})] - 1$
$1/2K_\lambda$ = $1/2K + (1+\tau)/\pi\lambda$
$2K$ = lift coefficient slope of the airfoil (or wing section, $\lambda \to \infty$)
$2K_\lambda$ = lift coefficient slope of the wing of aspect ratio λ, C_L/α_a

Subscripts

R, T = chord and incidence at the wing center (root, $y = 0$) and at the wing tip ($y = 1$)

Superscripts

A, S = coefficients of the antisymmetric and symmetric incidence variations, respectively

I. Introduction

THE flow past wings of finite span has been extensively studied over the past six decades for its application in the aerodynamic design. The classical lifting line theory developed by Prandtl and Glauert[1,2] established the foundation of the wing aerodynamics and provided the means for the computation of the aerodynamic forces, including the lift and induced drag. Numerous other methods of solution based on the lifting surface theory, on boundary element (or panel) methods, or using flowfield solvers based on various computational formulations, such as finite difference, finite volume, or finite element, have been developed for this problem in the last decades. Some of these methods (including those based on the lifting-line theory) are presented in books elaborated by Anderson,[2] Bisplinghoff et al.,[3] Carafoli,[4] Karamcheti,[5] Katz and Plotkin,[6] Katz,[7] Kuethe and Chow,[8] Milne-Thomson,[9] McCormick,[10] Robinson and Laurmann,[11] Schlichting and Truckenbrodt,[12] Thwaites,[13] Von Mises,[14] and others. Although recently developed methods provide good accuracy and can also take into account more complex wing features, methods based on the lifting-line theory are still used for a fast estimation of the spanwise load distribution and the basic aerodynamic characteristics of unswept wings. The lifting-line theories can also provide more physical insight of the influence of the wing geometrical shape and incidence variation on the overall aerodynamic forces (lift and induced drag) and on the spanwise distribution of local lift.

In classical lifting-line theory the wing is modeled by a spanwise-variable bound vortex and a sheet of free semi-infinite vortices; these are introduced to satisfy the Helmholtz vortex theorem. This leads to a mathematical formulation represented by a singular integro-differential equation, which relates the spanwise distribution of the circulation with the spanwise variations of the local wing chord and incidence via the normal-to-wing velocity component induced by the free vortex sheet. The indirect problems, with a specified circulation distribution, are more easily solved for the spanwise variation of one or the other of the local wing chord or the local incidence. However, the direct (physical) problem, which is the determination of the circulation distribution for specified spanwise variation of the wing shape and incidence, is more difficult to solve.

For the direct problem the classical lifting-line theory uses an infinite Fourier series expansion, which leads to an algebraic equation for the a priori unknown coefficients to be satisfied everywhere on the wing. This infinite series is eventually truncated to a finite number of terms, and the manner in which these unknown coefficients is determined distinguishes the numerous lifting-line methods that have been developed for this problem.

The most widely used schemes, such as that developed by Glauert,[1] are based on a collocation approach, which requires the resulting algebraic equation to be satisfied at an equal number of points along the wing span, leading to the solution of a linear system of algebraic equations. A more accurate approach using Gaussian quadratures has been developed by Multhopp.[15] However, the accuracy of the collocation methods depends substantially on the selection of the collocation points, especially when the wing chord and incidence have spanwise variations. Nevertheless, the collocation methods are most widely used and presented in recent aerodynamics books.[8,16]

Other methods[17–19] use variational formulations to determine the Fourier coefficients of the circulation, which avoids some of the difficulties encountered by the collocation methods.

Another interesting class of methods, such as those developed by Carafoli,[4,20] Karamcheti,[5] and Lotz,[21] uses Fourier expansions for the wing incidence and the inverse of the local chord. In particular, the method developed by Carafoli[4] is based on efficient cosine expansions of the inverse of the chord (with only three terms to appropriately represent the tapered wings) and uses a Fourier identification procedure to determine the Fourier coefficients of the circulation.

Recently, Rasmussen and Smith[22] developed a method based on a Fourier-series analysis to determine the coefficients of the infinite series expansion of the circulation. This method uses Fourier-series expansions for the spanwise variations of the local chord (not its inverse) and incidence in the case of right–left symmetry. The resulting infinite set of equations is then truncated to determine the first N unknown coefficients by solving an algebraic system of linear equations. For the same level of truncation, this method was found to converge faster and yield more accurate results than the collocation methods.

All of the lifting-line methods mentioned in the foregoing are directly based on the bound and free vortex scheme developed by Prandtl. They also use an infinite Fourier-series expansion of the spanwise variation of the circulation to express the integro-differential equation in algebraic form. The lifting-line methods use various schemes to reduce this algebraic equation (which should be satisfied everywhere on the wing span) to an infinite system of equations. This infinite system of equations is then truncated to a finite number N of equations to determine the first N unknown Fourier coefficients of the circulation. In all methods the truncation procedure is based on the assumption that the coefficients decrease monotonically with their rank, which is not always the case for various wing configurations (e.g., for several tapered wings the fourth coefficient is larger by an order of magnitude than the second and third ones, as calculated in Ref. 18, where a Fourier expansion truncated to four terms was considered).

In general, the Fourier-series expansions are not convenient for the wings with changes in the spanwise variation of the chord and/or incidence; these changes can be generated by the deflection of control surfaces located on the wing. In these cases a larger number of terms in the truncated Fourier expansions of the circulation is needed, and the solutions are less accurate and contain spurious spanwise oscillations. The inability of the Fourier-series expansions to model the sudden geometrical changes has been shown by Mateescu and Newman[23] (in Fig. 2, p. 791) for flapped airfoils.

The aim of this paper is to develop a new method of solution for the wings of finite span based on velocity singularities. (The term of velocity singularities was first introduced in Ref. 24.) The approach differs from the Prandtl and Glauert's lifting-line theory and the methods based on the Fourier-series expansion of the circulation. This new method more rigorously accounts for the sudden changes in the wing geometry and incidence variations (caused by the deflection of control surfaces along the wing span). New special functions are derived in this method to represent the contributions of these changes in the solution of the circulation. Thus the difficulties introduced by the use of Fourier-series expansions are avoided.

The methods based on velocity singularities determine the specific contributions in the velocity solution that are related to singular points on the wing or airfoil, where the boundary conditions change. These contributions are determined by taking into account the singular behavior of the fluid velocity at the singular points and satisfy all other boundary conditions (including Kutta condition at the trailing edge of an airfoil); these contributions are similar to the Green functions associated to these changes.

In subsonic flows, methods based on velocity singularities were first developed by Mateescu,[25] Mateescu and Nadeau,[26] and

Mateescu and Newman[23] for the analysis of the steady flows past rigid, flexible, or jet-flapped airfoils. More recently, velocity singularity methods have been also developed for the nonlinear aerodynamic analysis of airfoils (Mateescu[27]) and for the unsteady flows past oscillating airfoils (Mateescu and Abdo[28]). Methods based on velocity singularities have also been successfully developed for the analysis of wings and wing-body systems in supersonic flows (Mateescu[24]). In all of these subsonic and supersonic flow problems, the velocity singularity methods yield efficient theoretical solutions in closed form.

In this paper, for the analysis of finite-span wings, velocity singularities are considered on the trace of the free vortex sheet in the Trefftz crossflow plane (situated downstream at infinity), in contrast to the placement of velocity singularities directly on the airfoil[23,25,26] or on the wing.[24]

New special functions are derived in this method for the contributions caused by the changes in the wing incidence and chord variations in the solution of the circulation. The solutions contain both natural and forced symmetry and antisymmetry terms, which lead to a correct mathematical modeling of the physical problem. (The forced-symmetry terms were absent in the preceding methods using Fourier expansions.)

The method is first validated by comparison with the lifting-line solutions obtained by Rasmussen and Smith[22] for the rectangular and tapered wings of uniform incidence and with results obtained with a panel method (Katz and Plotkin[6]). Then this method is used to obtain efficient new solutions for wings with changes in the wing incidence and chord variations caused by symmetric and antisymmetric deflections of flaps and ailerons and for wings with curved leading and trailing edges and continuously variable incidence.

II. Method of Solution Based on Velocity Singularities

Consider an unswept thin wing of span $2b$ placed in a uniform stream of velocity U_∞. The wing geometry is defined by a specified spanwise variation of the local chord $bc(y)$, where $c(y)$ is the nondimensional local chord, and by a specified variation of the local wing incidence $\alpha(y)$, which includes the geometric incidence of the local wing section with respect to the velocity U_∞, and the added-by-camber incidence, representing the effect of the wing section camber (including also the effect of a local flap or aileron deflection).

The velocity components $v(y, z)$ and $w(y, z)$ along the y and z axes in the wing crossflow plane ($x = 0$), and the corresponding velocity components $v^*(y, z)$ and $w^*(y, z)$ in the Trefftz plane situated at $x \to \infty$, are harmonic functions in incompressible flows, satisfying the Laplace equation. Thus, a nondimensional complex conjugate velocity

$$U(X) = \frac{v^*(y, z) - i w^*(y, z)}{\alpha_a U_\infty} \tag{1}$$

can be defined in the Trefftz plane in function of the complex variable $X = y + iz$.

The circulation $\Gamma(y)$ around a wing section corresponds to the intensity of a bound vortex, which is variable along the span (as shown in Prandtl's vortex model). The spanwise variation of the intensity of this bound vortex is related (according to Helmholtz's vortex theorems) to a semi-infinite vortex sheet of distributed vortex intensity $\gamma(y) = \mathrm{d}\Gamma(y)/(b\,\mathrm{d}y)$, for $y \in (-1, 1)$. This local free vortex intensity $\gamma(y)$ is related to the spanwise velocity component $v^*(y, z)$ on the vortex sheet trace in the Trefftz plane (considering an infinitesimal control volume around a portion $b\,\mathrm{d}y$ of the free vortex sheet) in the form

$$v^*(y, 0) = \gamma(y)/2 \tag{2}$$

The vertical velocity component on the wing ($x = 0$), $w(y, z)$ is induced by this semi-infinite vortex sheet of intensity $\gamma(y)$, whereas the corresponding velocity component $w^*(y, z)$ in the Trefftz plane ($x \to \infty$) is induced by an infinite vortex sheet of the same intensity (according to Helmholtz's vortex theorem), and hence $w^*(y, z) = 2w(y, z)$.

In the aeronautical applications the wing chord and incidence variations can present sudden changes along the span. For example, sudden changes in the spanwise variation of the incidence can result from the designed wing twist, or from deflected control surfaces, such as the ailerons or flaps situated on the wing. These sudden incidence and/or chord changes induce changes in the variation of the velocity component $w^*(y, 0)$ on the trace of the free vortex sheet in the Trefftz plane.

Consider the general case of a wing with two such changes on the vortex sheet trace in the Trefftz plane located at $y = s_1$ and $y = -s_2$, defined by the boundary condition

$$\mathrm{IMAG}\{U(X)\}_{X=y} = -\bar{w}^*(y) \tag{3a}$$

$$\bar{w}^*(y) = W_0(y) + H(s_1, y)W_1(y) + H(s_2, -y)W_2(y) \tag{3b}$$

where $\bar{w}^*(y)$, $H(s_1, y)$, and $H(s_2, -y)$ are defined in the Nomenclature, and where $W_0(y)$, $W_1(y)$, and $W_2(y)$ are prescribed polynomial functions of y. Because $\gamma(y)$, and hence $v^*(y, 0)$, is zero outside the free vortex sheet, the additional boundary condition results:

$$\mathrm{REAL}\{U(X)\}_{X=y} = 0 \qquad \text{for} \quad y < -1 \quad \text{and} \quad y > 1 \tag{4}$$

This flow problem is similar to the two-dimensional incompressible flow past a thin plate characterized by the boundary conditions (3) and (4), which can be solved using the method of velocity singularities (see Refs. 23, 24, and 28).

A. Prototype Problem Solution

In the case when $W_0(y) = \beta_0$, $W_1(y) = \delta W_1$, and $W_2(y) = \delta W_2$ are constant (where δW_1 and δW_2 might or might not be infinitesimally small), the complex conjugate velocity $U(X)$ is characterized (as shown in previous papers[23,24,28]) by singularities located at the plate edges ($y = \pm 1$) and at the ridges $y = s_1$ and $y = -s_2$ (where the boundary conditions suddenly change): $(1 - X)^{-1/2}$, $(1 + X)^{-1/2}$, $\ell n(s_1 - X)$, and $\ell n(s_2 + X)$. Thus, the solution for the complex conjugate velocity can be obtained using the method of velocity singularities (see Refs. 23, 24, 28, and 29) in the form

$$U(X) = i\beta_0 + \frac{A_0 + AX}{\sqrt{1 - X^2}} - \delta W_1 \tilde{G}(s_1, X) + \delta W_2 \tilde{G}(s_2, -X) \tag{5}$$

where $\tilde{G}(s_1, X)$ and $\tilde{G}(s_2, -X)$ represent the singular contributions of the ridges situated at $y = s_1$ and $y = -s_2$, respectively, and are defined in the Nomenclature. The second term of the right-hand side represents the singular contributions of the plate edges (corresponding to the wing tips). The constants A and A_0 are determined from the conditions $[U(X)]_{X \to \infty} = 0$ and $\bar{\Gamma}(1) = \bar{\Gamma}(-1) = 0$, where the nondimensional circulation $\bar{\Gamma}(y) = \Gamma(y)/[2b\alpha_a U_\infty]$ on the wing trace in the Trefftz plane is obtained from Eqs. (1) and (2) as

$$\bar{\Gamma}(y) = -\int_y^1 \mathrm{REAL}[U(X)]_{X=y}\,\mathrm{d}y \tag{6}$$

Thus, for A, A_0, and $\bar{\Gamma}(y)$ the following expressions result:

$$A = \beta_0 + \delta W_1 C(s_1) + \delta W_2 C(s_2) \tag{7}$$

$$A_0 = \left[\delta W_1 \sqrt{1 - s_1^2} - \delta W_2 \sqrt{1 - s_2^2}\right]\Big/\pi \tag{8}$$

$$\bar{\Gamma}(y) = A\sqrt{1 - y^2} + \delta W_1 (y - s_1) G(s_1, y) - \delta W_2 (y + s_2) G(s_2, -y) \tag{9}$$

where $G(s_1, y)$ and $G(s_2, -y)$, which represent the real parts of $\tilde{G}(s_1, X)$ and $\tilde{G}(s_2, -X)$ for $X = y$, and $C(s)$ are defined in the Nomenclature.

B. Complete Problem Solution

For the general wing problem defined by Eq. (3), the sudden changes in the boundary conditions at $y = s_1$ and $y = -s_2$ are represented by the ridge contributions $W_1(s_1)\tilde{G}(s_1, X)$ and $W_2(s_2)\tilde{G}(s_2, -X)$ in $U(X)$. The variation of the boundary condition (3) related to $W_0(y)$ can be modeled by a continuous distribution of elementary ridges defined by the contributions $[W_0'(\sigma)\,d\sigma]\tilde{G}(\sigma, X)$ and respectively $[-W_0'(-\sigma)\,d\sigma]\tilde{G}(\sigma, -X)$ for $0 < \sigma < 1$. The variations related to $W_1(y)$ and $W_2(y)$ can be modeled by two continuous distributions of elementary ridges defined by the contributions $[W_1'(\sigma)\,d\sigma]\tilde{G}(\sigma, X)$ for $s_1 < \sigma < 1$ and $[-W_2'(-\sigma)\,d\sigma]\tilde{G}(\sigma, -X)$ for $s_2 < \sigma < 1$, respectively. Thus, one obtains

$$\bar{\Gamma}(y) = \int_0^1 [W_0(\sigma)G(\sigma, y) + W_0(-\sigma)G(\sigma, -y)]\,d\sigma + \int_{s_1}^1 W_1(\sigma)G(\sigma, y)\,d\sigma + \int_{s_2}^1 W_2(-\sigma)G(\sigma, -y)\,d\sigma \tag{10}$$

The general polynomial representations for the functions $W_0(y)$, $W_1(y)$, and $W_2(y)$ on the vortex sheet trace in the Trefftz plane are

$$W_0(y) = \sum_{k=0}^{2n} \beta_k y^k, \qquad W_1(y) = \sum_{k=0}^{\hat{n}} \beta_k^1 y^k, \qquad W_2(y) = \sum_{k=0}^{\hat{n}} \beta_k^2 y^k \tag{11}$$

where in general $\beta_k = \beta_k^S + \beta_k^A$ for $y > 0$ and $\beta_k = (-1)^k(\beta_k^S - \beta_k^A)$ for $y < 0$, in which the superscripts S and A correspond respectively to the symmetric and antisymmetric variations of the wing incidence (which refers to the right–left symmetry).

The general solution of the nondimensional circulation $\bar{\Gamma}(y)$ on the wing can thus be obtained as

$$\bar{\Gamma}(y) = \sum_{k=0}^{n} \left[\beta_k^S F_k^0(y) + \beta_k^A F_k^1(y)\right] + \sum_{k=0}^{\hat{n}} \left[\hat{\beta}_k^1 \hat{F}_k(s_1, y) + (-1)^k \hat{\beta}_k^2 \hat{F}_k(s_2, -y)\right] \tag{12}$$

$$F_k^r(y) = \ell_{k+r+1}\frac{2y^{k+1}}{k+1}G_0(y) + \frac{\sqrt{1-y^2}}{k+1}\sum_{j=0}^{k} \ell_{j+r} I_{k-j} y^j \tag{12a}$$

$$\hat{F}_k(s, y) = \frac{y^{k+1} - s^{k+1}}{k+1}G(s, y) + \frac{\sqrt{1-y^2}}{2(k+1)}\sum_{j=0}^{k} J_{k-j}(s) y^j \tag{12b}$$

where $G_0(y)$, $G(s, y)$, ℓ_k, I_j, and $J_j(s)$ are defined in the Nomenclature.

The general solution (12) of the spanwise variation of the circulation was obtained for an arbitrary wing geometry and for a general spanwise variation of the incidence. The latter includes both symmetric and antisymmetric incidence variations with respect to the central chord, with or without sudden changes on the wing caused by the deflection of the control surfaces (such as flaps and ailerons). This general solution includes all cases of the natural and forced symmetry and antisymmetry of the wing chord and incidence variations.

The new functions $F_k^0(y)$ and $F_k^1(y)$, corresponding to the superscripts $r = 0$ and 1, take into account the continuous symmetric and antisymmetric variations of the wing incidence. They include the function $G_0(y)$, which takes into account the discontinuities at $y = 0$ that are introduced by the forced symmetry (and antisymmetry) terms in the wing chord and incidence variations. The forced symmetry terms are not considered in the preceding methods, although they clearly have an effect on the spanwise distribution of the circulation for tapered wings, which is not continuous at $y = 0$ (in contrast to the rectangular wings), as shown in Sections III and V.B.

The new functions $\hat{F}_k(s_1, y)$ and $\hat{F}_k(s_2, -y)$ in the general solution (12) take into account the changes in the wing incidence and chord at $y = s_1$ and $y = -s_2$ (related to the deflection of the control surfaces located on the wing). These specific contributions related to the wing discontinuities, derived here for the first time, are not taken into account in the earlier methods using Fourier expansions of the circulation, as the Fourier expansions are not suited to model aerodynamic discontinuities.[23]

C. Determination of the Coefficients β_k

To determine the unknown coefficients β_k, consider the following expression of the local nondimensional circulation around the wing section $\bar{\Gamma}_L(y)$, which depends on the effective incidence $\alpha_{\text{eff}}(y) = \alpha(y) - w(y, 0)/U_\infty = \alpha_a[\bar{\alpha}(y) - \bar{w}^*(y)/2]$:

$$\bar{\Gamma}_L(y) = \tfrac{1}{2}Kc_a\bar{c}(y)\left[\bar{\alpha}(y) - \tfrac{1}{2}\bar{w}^*(y)\right] \tag{13}$$

where $\bar{w}^*(y)$ and $\bar{\alpha}(y)$ are defined in the Nomenclature, and $K = C_{L\alpha}/2$ is half of the lift coefficient slope ($C_{L\alpha} = dC_L/d\alpha$). Thin airfoil theory gives $K = \pi$, and Carafoli[4] recommends $K = (0.85 - 0.95)\pi$ to include the viscous effects on the lift coefficient slope.

The equality of expressions (12) and (13) of the circulation at any location along the span yields an equation that can be used to determine the unknown coefficients β_k: $\bar{\Gamma}(y) = \bar{\Gamma}_L(y)$.

To determine the coefficients β_k, one might use the collocation method (which was extensively used in the lifting-line methods based on Fourier expansions) by imposing the preceding equality to be satisfied at specified locations along the wing span, in order to obtain a system of linear equations for β_k. However, the accuracy of the solution provided by the collocation procedure (which usually leads to spurious oscillations) is not very good, especially in the case of sudden changes in the wing geometry and incidence variations, when the selection of the collocation points becomes a challenging process.

1. *Present Solution Procedure*

A special procedure similar to the Galerkin technique is developed in order to obtain an enhanced accuracy of the solution. In this procedure a system of $N + 1$ linear equations (with the same number of unknown coefficients β_k) is obtained by multiplying the equation $\bar{\Gamma}(y) = \bar{\Gamma}_L(y)$ with y^i, where $i \in \{0, 1, \ldots, N\}$, and integrating along the wing span:

$$\int_{-1}^{1} \bar{\Gamma}(y) y^i\,dy = \int_{-1}^{1} \bar{\Gamma}_L(y) y^i\,dy \tag{14}$$

In contrast to the collocation method, Eq. (14) yields a better resolution of the incidence variation and wing geometry and a better accuracy for a given number of unknown coefficients. To formally justify this improved solution procedure, one can note that the polynomial terms can be expressed as a sum of Tchebyshev polynomials

$$y^i = \frac{1}{2^i}\sum_{k=0}^{n} C_i^k T_{i-2k}(y)$$

where C_i^k are the binomial coefficients. Thus, the system of equations (14) is equivalent to the system of equations

$$\int_{-1}^{1} [\bar{\Gamma}(y) - \bar{\Gamma}_L(y)] T_i(y)\,dy = 0$$

where the Tchebyshev polynomials $T_i(y)$ are used as orthogonal test functions.

It is also worth noting that the integrals appearing in Eq. (14) are also present in the calculation of the lift coefficient (those for $i = 0$) and the induced drag coefficient (those for $i \geq 0$) because $\bar{w}^*(y)$ has a polynomial representation defined by Eqs. (3) and (11). This enhances the accuracy of the improved solution approach and simplifies the calculation of the aerodynamic characteristics of the wing by using the simpler expression $\bar{\Gamma}_L(y)$ of the circulation, instead of $\bar{\Gamma}(y)$, which usually is more complicated.

2. Aerodynamic Characteristics

The lift and induced drag coefficients C_L and C_{Di} can thus be calculated using $\bar{\Gamma}_L(y)$ by the equations

$$C_L = \lambda\alpha_a \int_{-1}^{1} \bar{\Gamma}_L(y)\,\mathrm{d}y, \qquad C_L = 2K(\alpha_a - \alpha_{ia}) \tag{15a}$$

$$C_{\mathrm{Di}} = \lambda\alpha_a^2 \int_{-1}^{1} \frac{1}{2}\bar{w}^*(y)\bar{\Gamma}_L(y)\,\mathrm{d}y, \qquad C_{\mathrm{Di}} = 2K\alpha_a^2\delta^* \tag{15b}$$

$$\alpha_{ia} = \alpha_a\alpha_{ia}^*, \qquad \alpha_{ia}^* = \frac{1}{2}\int_{-1}^{1} \bar{c}(y)\frac{1}{2}\bar{w}^*(y)\,\mathrm{d}y \tag{15c}$$

$$\delta^* = \frac{1}{2}\int_{-1}^{1} \bar{c}(y)\frac{1}{2}\bar{w}^*(y)\left[\bar{\alpha}(y) - \frac{1}{2}\bar{w}^*(y)\right]\mathrm{d}y \tag{15d}$$

where the wing aspect ratio λ is defined in the Nomenclature. By analogy with the elliptic wing, one can define

$$C_L = 2K_\lambda\alpha_a, \qquad 1/2K_\lambda = 1/2K + (1+\tau)/\pi\lambda \tag{16a}$$

$$C_{\mathrm{Di}} = \left(C_L^2/\pi\lambda\right)(1+\delta), \qquad \alpha_{ia} = (C_L/\pi\lambda)(1+\tau) \tag{16b}$$

where $2K_\lambda$ and $2K$ are the lift coefficient slopes for the wing of aspect ratios λ and for a two-dimensional airfoil ($\lambda \to \infty$), respectively. The lift and induced-drag factors τ and δ are

$$\tau = (\pi\lambda/2K)\left[\alpha_{ia}^*/\left(1-\alpha_{ia}^*\right)\right] - 1$$

$$\delta = (\pi\lambda/2K)\left[\delta^*/\left(1-\alpha_{ia}^*\right)^2\right] - 1 \tag{17}$$

III. Solutions for Symmetric Wings with Continuous Incidence Variation

Consider the general symmetric variation of the wing chord and incidence in the form

$$\bar{c}(y) = \sum_{m=0}^{n_m} \bar{c}_m|y|^m, \qquad \bar{\alpha}(y) = \sum_{j=0}^{n_i} \bar{\alpha}_j|y|^j \tag{18}$$

which can represent any continuous variation of the chord and incidence along the wing span, including the case of the wings with curved leading edges. For symmetric wings ($\beta_k^A = 0$ and $\beta_k^S = \beta_k$) the general solution (12) is substantially simplified to

$$\bar{\Gamma}(y) = \sum_{k=0}^{2n} \beta_k F_k^0(y) \tag{19}$$

This solution includes both the even and odd terms in k that correspond to the natural and forced symmetry terms, respectively. This ensures a correct and more general mathematical formulation of the physical problem, for example, the chord variation of tapered wings contains a forced symmetry term $c(y)/c_R = 1 \mp qy$, where the upper and lower signs refer to the right and left sides, respectively. Moreover, by considering both even and odd terms the highest order $k = 2n$ for the same number of coefficients β_k is substantially reduced (by almost a half). This avoids the presence of spurious oscillations in the solution of the spanwise variation of the circulation, in contrast to the methods that use Fourier series restricted only to the even (natural-symmetry) terms.

The functions $F_k^0(y)$ contain, as shown in Eqs. (12), the function $G_0(y)$, which takes into account the geometrical discontinuities at $y = 0$ (as in the case of the chord variation slope for trapezoidal wings), which are associated with the forced symmetry terms.

Equation (14) is used to determine the coefficients β_k. This is written as a system of $N = 2n + 1$ linear equations in matrix form, for $i \in \{0, 1, \ldots, 2n\}$ and $k \in \{0, 1, \ldots, 2n\}$:

$$\{B_{i,k}\}[\beta_k] = [D_i] \tag{20a}$$

$$B_{i,k} = E_{i,k} + \frac{\pi}{k+1}\sum_{j=0}^{k} \ell_j I_{k-j} P_{j+i} + \frac{2\ell_{k+1}}{k+1}\frac{I_{k+i+1}}{k+i+2} \tag{20b}$$

$$D_i = Kc_a \sum_{m=0}^{n_m}\sum_{j=0}^{n_j} \frac{\bar{c}_m\bar{\alpha}_j}{m+j+i+1} \tag{20c}$$

$$E_{i,k} = \frac{K}{2}c_a \sum_{m=0}^{n_m} \frac{\bar{c}_m}{m+k+i+1}, \qquad P_k = \frac{I_k}{(k+2)} \tag{20d}$$

The aerodynamic coefficients can then be determined from Eqs. (16), where α_{ia}^* and δ^* are

$$\alpha_{ia}^* = \frac{1}{2}\sum_{m=0}^{n_m}\sum_{k=0}^{2n} \frac{\bar{c}_m\beta_k}{k+m+1} \tag{21a}$$

$$\delta^* = \frac{1}{2}\sum_{m=0}^{n_m}\sum_{k=0}^{2n} \bar{c}_m\beta_k\left[\sum_{j=0}^{n_j}\frac{\bar{\alpha}_j}{k+m+j+1} - \frac{1}{2}\sum_{j=0}^{2n}\frac{\beta_j}{k+m+j+1}\right] \tag{21b}$$

A. Solutions for Rectangular and Tapered Wings: Method Validation

The present method was validated by considering the flow over flat rectangular and tapered wings. The geometry of the flat trapezoidal wing of taper ratio q is defined by $c(y) = c_R(1-q|y|)$, $\alpha(y) = \alpha_a = \alpha_R$, $c_a = (1-q/2)c_R = 2/\lambda$, $\bar{c}_0 = c_R/c_a = 1/(1-q/2)$, $\bar{c}_1 = -q\bar{c}_0$, and $\bar{\alpha}_0 = 1$. In this case the coefficients D_i and $E_{i,k}$ defined in Eqs. (20) are

$$D_i = Kc_a[\bar{c}_0/(i+1) + \bar{c}_1/(i+2)] \tag{22a}$$

$$E_{i,k} = Kc_a[\bar{c}_0/(k+i+1) + \bar{c}_1/(k+i+2)]/2 \tag{22b}$$

where $K = \pi$ is used in most of the following numerical examples.

The present solutions for the spanwise variation of the circulation $\bar{\Gamma}(y)$ and the lift and induced drag factors τ and δ are compared in Tables 1 and 2, for the purpose of validation, with the results obtained by Rasmussen and Smith[22] for a rectangular wing ($q = 0$) of aspect ratio $\lambda = 6$ and for a trapezoidal wing of taper ratio $q = 0.6$ and $\lambda = 9$. For a more meaningful comparison in the same tables are also given the results obtained with a panel method (Katz and Plotkin[6]) for $I = 8$ panels along the chord and $J = 10$ panels along the wing semispan (or 20 panels along wing span), and for this reason the values of $\bar{\Gamma}(y)$ are given at the panel centers. (The solutions calculated with $J = 20$ panels displayed very small changes compared with $J = 10$.)

The present solutions based on velocity singularities are in very good agreement with the results of Rasmussen and Smith[22] for both the rectangular and trapezoidal wings. The present solutions obtained with $n = 5$ show a very good accuracy, although those for $n = 3$ and 4 are also accurate (even $n = 1$ provides an acceptable engineering accuracy). This can also be seen from the average relative differences ε_Γ between these solutions for $\bar{\Gamma}(y)$ and the relative differences for the lift and induced-drag coefficients ε_L and ε_D also shown in these tables. The spanwise variation of $\bar{\Gamma}(y)$ in the present solutions is smoother than in the Rasmussen and Smith solution, which has slight oscillations especially near the central chord (e.g., the values at $y = 0.05$ were slightly larger than those at $y = 0$, instead of smaller); this is probably caused by the absence of the forced symmetry terms. The effect of the forced symmetry terms in the circulation distribution, which is not continuous at $y = 0$, can be seen in Fig. 1 (and more clearly in Sec. VB, which including both the right and the left sides of the wing). For trapezoidal wings the present solutions were found to be slightly closer to the panel method results (Katz and Plotkin[6]) than Rasmussen and Smith solutions were.

The variations with the wing taper ratio q of the lift and induced drag factors τ and δ calculated with $n = 5$ for four values of the aspect ratio λ are compared in Fig. 2 with the panel method results (Katz and Plotkin[6]). A good agreement is found between the present solutions and the panel method results, especially for $\lambda > 3$ (even

Table 1 Values of $\bar{\Gamma}(y)$, τ, and δ for a rectangular wing ($q = 0$) of $\lambda = 6$

	Present solution of $\bar{\Gamma}(y)$					Panel method Katz and Plotkin[6]	Rasmussen and Smith[22]
y	$n=1$	$n=2$	$n=3$	$n=4$	$n=5$	$I=8, J=10$	8-term
0.00	0.4396	0.4332	0.4323	0.4321	0.4320	——	0.4312
0.05	0.4377	0.4319	0.4315	0.4316	0.4317	0.4285	0.4317
0.15	0.4299	0.4289	0.4303	0.4304	0.4302	0.4269	0.4303
0.25	0.4214	0.4268	0.4274	0.4267	0.4269	0.4234	0.4270
0.35	0.4143	0.4231	0.4214	0.4215	0.4217	0.4184	0.4214
0.45	0.4084	0.4152	0.4130	0.4139	0.4135	0.4107	0.4135
0.55	0.4018	0.4019	0.4021	0.4019	0.4020	0.3996	0.4021
0.65	0.3909	0.3829	0.3855	0.3845	0.3848	0.3821	0.3847
0.75	0.3687	0.3564	0.3580	0.3583	0.3579	0.3554	0.3579
0.85	0.3217	0.3140	0.3117	0.3124	0.3127	0.3104	0.3127
0.95	0.2106	0.2150	0.2139	0.2131	0.2127	0.2118	0.2127
τ	0.1481	0.1589	0.1602	0.1605	0.1606	0.1635	0.1606
δ	0.0540	0.0495	0.0486	0.0484	0.0483	0.0474	0.0483
$C_{L\alpha}$	4.5442	4.5323	4.5309	4.5306	4.5305	4.5273	4.5305
C_{Di}	1.1547	1.1438	1.1420	1.1416	1.1415	1.1390	1.1415
ε_Γ, %	0.453	0.124	0.052	0.026	0.015	−0.635	——
ε_L, %	0.302	0.040	0.009	0.002	0.000	−0.070	——
ε_D, %	1.156	0.198	0.046	0.013	0.003	−0.223	——

Table 2 Values of $\bar{\Gamma}(y)$, τ, and δ for a trapezoidal wing of $q = 0.6$ and $\lambda = 9$

	Present solution of $\bar{\Gamma}(y)$					Panel method Katz and Plotkin[6]	Rasmussen and Smith[22]
y	$n=1$	$n=2$	$n=3$	$n=4$	$n=5$	$I=8, J=10$	8-term
0.00	0.3813	0.3775	0.3765	0.3762	0.3761	——	0.3735
0.05	0.3782	0.3741	0.3737	0.3738	0.3740	0.3724	0.3737
0.15	0.3633	0.3622	0.3638	0.3639	0.3636	0.3625	0.3643
0.25	0.3441	0.3486	0.3492	0.3483	0.3486	0.3470	0.3486
0.35	0.3244	0.3324	0.3300	0.3304	0.3305	0.3291	0.3299
0.45	0.3053	0.3116	0.3089	0.3101	0.3095	0.3089	0.3098
0.55	0.2868	0.2863	0.2871	0.2866	0.2869	0.2855	0.2871
0.65	0.2674	0.2586	0.2625	0.2611	0.2614	0.2600	0.2611
0.75	0.2432	0.2306	0.2322	0.2331	0.2324	0.2320	0.2325
0.85	0.2061	0.1998	0.1958	0.1966	0.1973	0.1957	0.1973
0.95	0.1321	0.1400	0.1391	0.1376	0.1368	0.1376	0.1369
τ	0.03231	0.04711	0.05044	0.05127	0.05153	0.05250	0.0514
δ	0.01353	0.01670	0.01583	0.01538	0.01521	0.01494	0.0152
$C_{L\alpha}$	5.1108	5.0971	5.0941	5.0933	5.0931	5.0922	5.0932
C_{Di}	0.9363	0.9342	0.9323	0.9316	0.9314	0.9308	0.9314
ε_Γ, %	0.536	0.280	0.150	0.084	−0.033	−0.300	——
ε_L, %	0.345	0.077	0.017	0.002	−0.002	−0.020	——
ε_D, %	0.526	0.303	0.097	0.023	−0.003	−0.065	——

for triangular wings $q = 1$). One can notice that the induced drag of the trapezoidal wings with a taper ratio between $q = 0.6$ and 0.65 is very close to the minimum induced drag of the elliptic wings (for which $\delta = 0$).

The influence of the aspect ratio λ on the spanwise distribution of the circulation is shown in Fig. 1 for rectangular ($q = 0$) and trapezoidal ($q = 0.6$) wings. The influence of the wing taper ratio q on the spanwise variation of the local lift coefficient $C_l(y)/C_L = (2/K_\lambda)\bar{\Gamma}(y)/c(y)$ is illustrated in Fig. 3a for $\lambda = 9$, and the variation of the lift coefficient slope $C_{L\alpha} = 2K_\lambda$ in function of q for four values of λ is shown in Fig. 3b. A comparison between the spanwise varitions of the circulation $\bar{\Gamma}(y)$ for tapered wings of various values of the taper ratio q and elliptic wings is illustrated in Fig. 4 for $\lambda = 2K$, where $K = 0.9\pi$ was used to take into account the viscous effects on the lift coefficient slope, as recommended by Carafoli.[4] Good agreement is found between the present solutions and the results of Carafoli.[4]

B. Wings with Curved Leading and Trailing Edges and Variable Incidence

The solution (19) of the circulation $\bar{\Gamma}(y)$, as well as the general solution (12), includes also the case of curved leading and trailing edges with a variable incidence along the span. Wings with curved edges are more difficult to be modeled using panel methods (and in general by numerical methods), but they are easily solved with the present method.

The solution (19) for wings with curved leading and trailing edges is illustrated for a wing with a parabolic chord variation $c(y) = c_R(1 - qy^2)$, $c_a = (1 - q/3)c_R = 2/\lambda$, $\bar{c}_0 = 1/(1 - q/3)$, and $\bar{c}_2 = -q\bar{c}_0$. Two incidence variations have been considered for this wing: 1) a parabolic incidence variation $\alpha(y) = \alpha_R(1 + ay^2)$, for which $\bar{\alpha}_0 = \alpha_R/\alpha_a = (3 - q)/(3 - q + a - 3qa/5)$ and $\bar{\alpha}_2 = a\bar{\alpha}_0$; and 2) a uniform incidence $\alpha(y) = \alpha_a = \alpha_R$, with $\bar{\alpha}_0 = 1$ (which corresponds to $a = 0$).

The solutions obtained for these wings are shown in Fig. 5 for $\lambda = 9$ and $q = 0.6$. Three cases of parabolic incidence variation ($a = 0$, 0.4, and 0.8) are considered. The nondimensional circulation $\bar{\Gamma}_R(y) = \Gamma(y)/[2b\alpha_R U_\infty]$ is used to compare the influence of the incidence variation. The solution for a trapezoidal wing of uniform incidence α_R with the same root chord c_R and taper ratio $q = 0.6$ [corresponding to the aspect ratio $\lambda = 9(1 - q/2)/(1 - q/3)$] is also shown for comparison. As expected, the circulation $\bar{\Gamma}_R(y)$ for the trapezoidal wing is smaller than that of the wing with curved leading and trailing edges of the same incidence α_R.

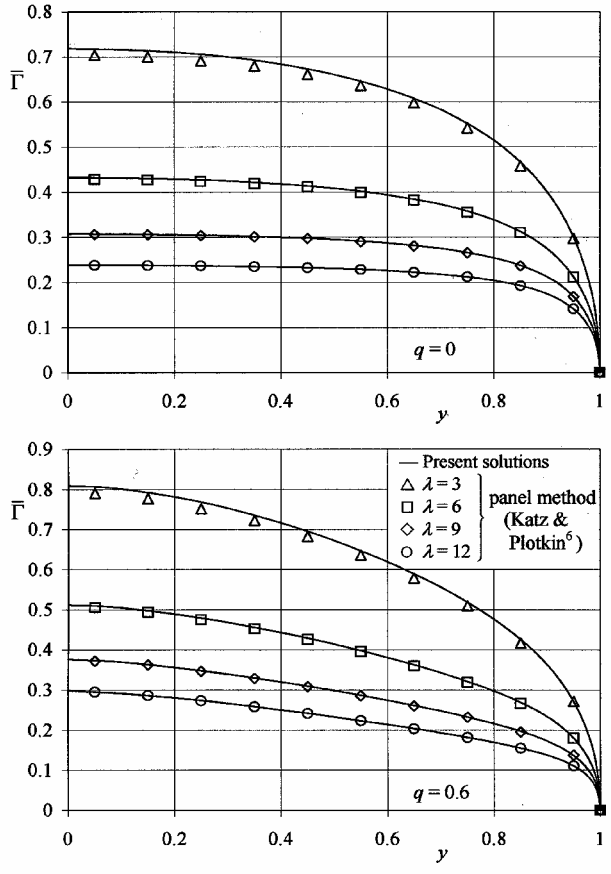

Fig. 1 Tapered wings: influence of the aspect ratio λ on the distribution of $\bar{\Gamma}(y)$.

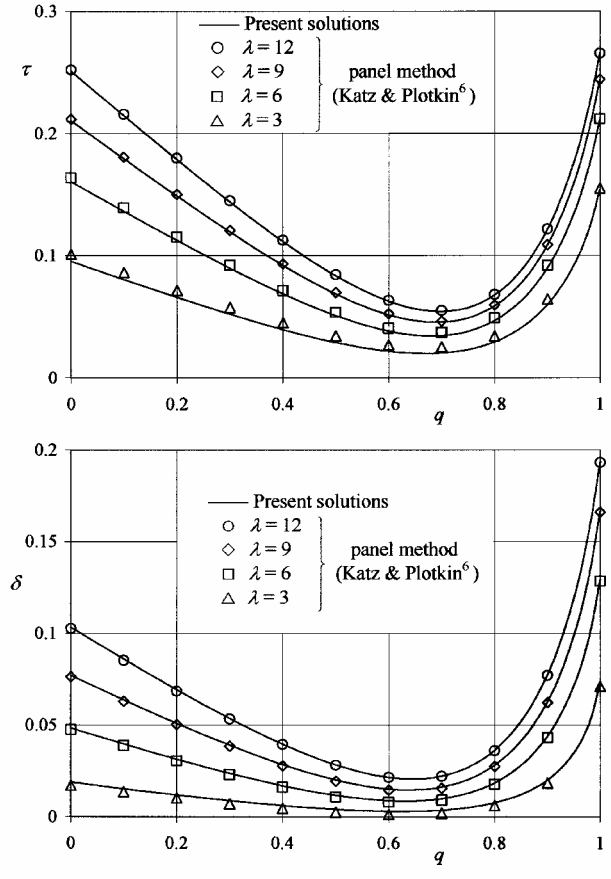

Fig. 2 Tapered wings: variation of τ and δ with the taper ratio q for various aspect ratios λ.

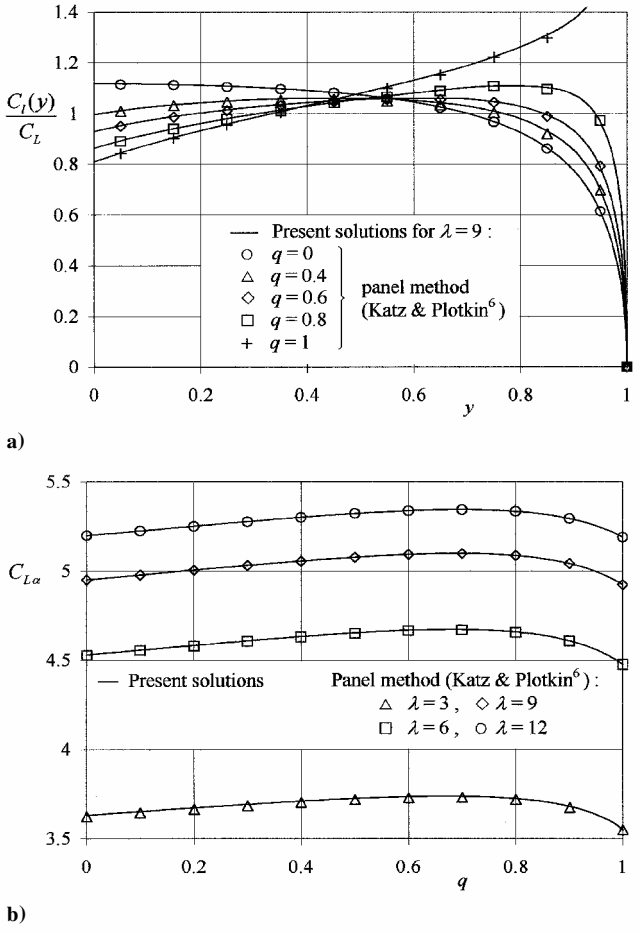

Fig. 3 Influence of the taper ratio q on a) local lift coefficient distribution $C_l(y)/C_L$ for $\lambda = 9$ and b) variation of the lift coefficient slope $C_{L\alpha} = 2K_\lambda$ for various λ.

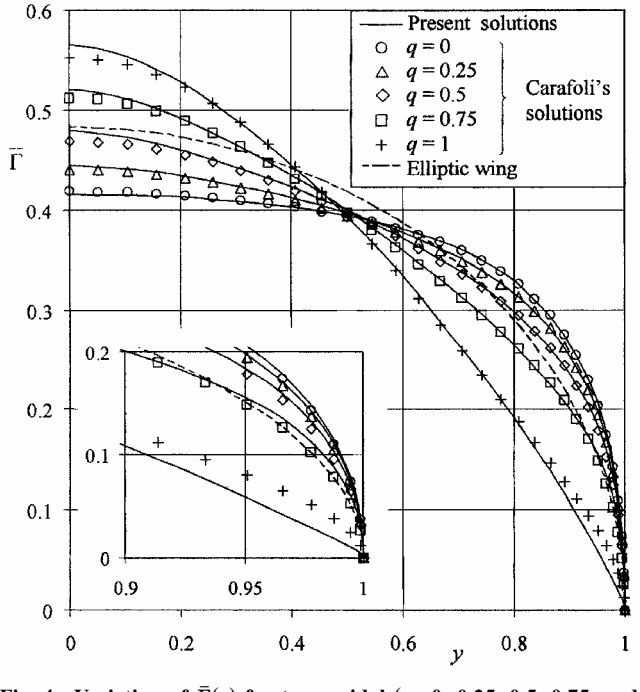

Fig. 4 Variation of $\bar{\Gamma}(y)$ for trapezoidal ($q = 0$, 0.25, 0.5, 0.75, and 1) and elliptic wings. Comparison with Carafoli's solutions for uniform wing incidence.

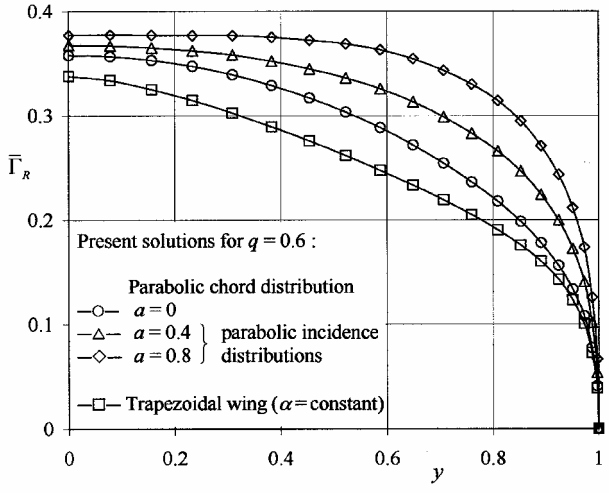

Fig. 5 Wings with curved edges and variable incidence—parabolic chord distribution: variation of $\bar{\Gamma}_R(y) = \Gamma(y)/[2b\alpha_R U_\infty]$ along span.

IV. Solutions for Symmetric Wings with Incidence and Chord Changes

A. General Case

In many cases the wings have sudden changes in the spanwise variations of the geometrical shape (chord variation) and incidence. The latter is usually as a result of the deflection of control surfaces located on the wing, such as ailerons or flaps. Consider such a symmetric wing with sudden changes of incidence and/or geometry occurring at $y = s$ and $y = -s$ defined by

$$\bar{c}(y) = \sum_{m=0}^{n_m} \left[\bar{c}_m + H(s, y)\bar{c}^*_m + H(s, -y)\bar{c}^*_m\right]|y|^m \quad (23a)$$

$$\bar{\alpha}(y) = \sum_{j=0}^{n_i} \left[\bar{\alpha}_j + H(s, y)\bar{\alpha}^*_j + H(s, -y)\bar{\alpha}^*_j\right]|y|^j \quad (23b)$$

where $H(s, y)$ and $H(s, -y)$ are defined in the Nomenclature. In this case ($\beta^A_k = 0$, $\beta^S_k = \beta_k$, $\hat{\beta}^1_k = (-1)^k\hat{\beta}^2_k = \hat{\beta}_k$), the simplification of the general solution (12) yields

$$\bar{\Gamma}(y) = \sum_{k=0}^{2n} \beta_k F^0_k(y) + \sum_{k=0}^{\hat{n}} \hat{\beta}_k[\hat{F}_k(s, y) + \hat{F}_k(s, -y)] \quad (24)$$

The new functions $\hat{F}_k(s, y) + \hat{F}_k(s, -y)$ represent the specific contributions of the symmetric changes in the wing incidence and chord at $y = s$ and $y = -s$.

The unknown coefficients β_k are determined from the system of equations (in matrix form)

$$\{B_{i,k} + \breve{B}_{i,k}\}[\beta_k] + \left\{B^*_{i,k}\right\}[\hat{\beta}_k] = \left[D_i + D^*_i\right] \quad (25a)$$

$$\breve{B}_{i,k} = \frac{K}{2}c_a \sum_{m=0}^{n_m} \bar{c}^*_m \frac{1 - s^{m+k+i+1}}{m+k+i+1} \quad (25b)$$

$$B^*_{i,k} = E^*_{i,k} + \frac{\pi}{k+1}\sum_{j=0}^{k} \ell_j J_{k-j}(s) P_{j+i} - 2g_{i.1}\frac{s^{k+i+2}}{k+i+2}G_0(s) + \frac{\sqrt{1-s^2}}{k+i+2}\left(\frac{2}{k+1}\sum_{j=0}^{k} \ell_{j+1} I_{j+i+1} s^{k-j} - \sum_{j=0}^{i} g_{i,j} I_j s^{k+1+i-j}\right) \quad (25c)$$

$$D^*_i = Kc_a \sum_{m=0}^{n_m}\sum_{j=0}^{n_j} \left[\bar{c}_m\bar{\alpha}^*_j + \bar{c}^*_m\left(\bar{\alpha}_j + \bar{\alpha}^*_j\right)\right]\frac{1 - s^{m+j+i+1}}{m+j+i+1} \quad (25d)$$

$$E^*_{i,k} = \frac{K}{2}c_a \sum_{m=0}^{n_m}\left(\bar{c}_m + \bar{c}^*_m\right)\frac{1 - s^{m+k+i+1}}{m+k+i+1} \quad (25e)$$

where $B_{i,k}$ and D_i are defined in Eqs. (20).

B. Trapezoidal and Rectangular Wings with Symmetric Incidence Changes

The solution (24) of the spanwise variation of $\bar{\Gamma}(y)$ is illustrated in Fig. 6 for the case of rectangular ($q = 0$) and trapezoidal ($q = 0.6$) wings. These wings have sudden changes of incidence from α_R to α_T at $y = \pm s = \pm 0.5$. For a meaningful comparison the wing solutions compared in Fig. 6 correspond to the same average (mean) incidence α_a, and hence $\bar{\alpha}_T = \alpha_T/\alpha_a$ and $\bar{\alpha}_R = \alpha_R/\alpha_a$ are related by $\bar{\alpha}_T = \bar{\alpha}_R + (1 - \bar{\alpha}_R)(2 - q)/[(1 - s)(2 - q - qs)]$.

The present solutions for $\lambda = 9$ (calculated with $n = 3$ and $\hat{n} = 4$) are in very good agreement with the panel method (Katz and Plotkin[6]) results.

This shows the utility of the functions $\hat{F}_k(s, y) + \hat{F}_k(s, -y)$ to represent the contributions of the symmetric changes in the chord and incidence variations. The Fourier series used in the preceding methods are not capable of accurately modeling these sudden changes.

The influence of the location of sudden changes in incidence, $s = 0.4$, 0.5 and 0.6, is shown in Fig. 7 for rectangular ($q = 0$) and trapezoidal ($q = 0.6$) wings of aspect ratio $\lambda = 9$ and $\alpha_R = 0$. The nondimensional circulation $\bar{\Gamma}_T(y) = \Gamma(y)/[2b\alpha_T U_\infty]$ is used in this case. The present solutions are found in good agreement with the panel method (Katz and Plotkin[6]) results.

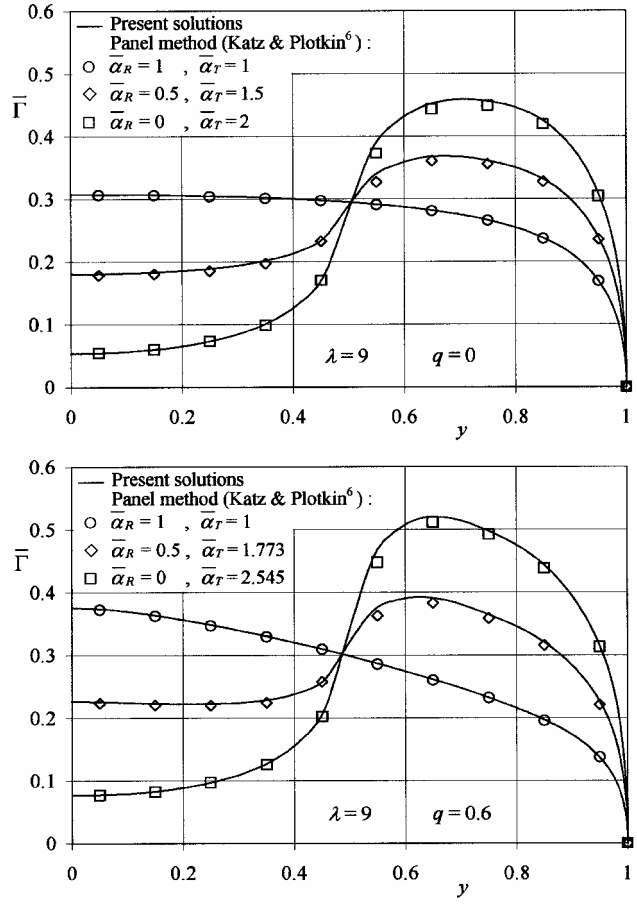

Fig. 6 Symmetric wings with incidence changes caused by control surface deflection (flaps): variation of $\bar{\Gamma}(y)$ along span.

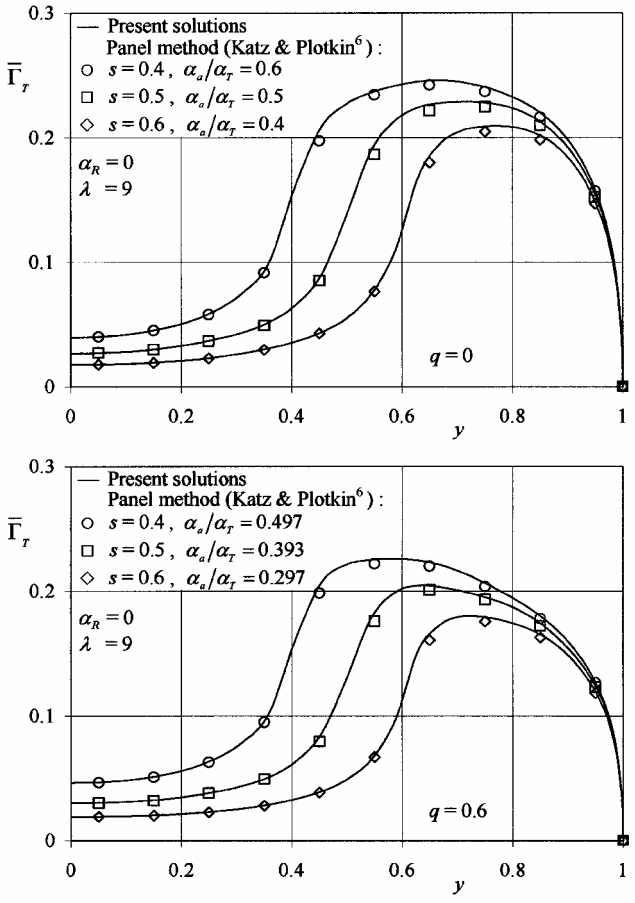

Fig. 7 Symmetric wings with incidence changes caused by control surface deflection (flaps): influence of the location s of incidence changes on the variation of $\bar{\Gamma}_T(y) = \Gamma(y)/[2b\alpha_T U_\infty]$.

V. Solutions for Wings with Asymmetric Incidence Variation

A. Wings with Antisymmetric Incidence Variation

1. General Case

The wing incidence might have an antisymmetric variation of incidence, either continuous, such as $\alpha(y) = \alpha_T y$ (which might correspond to the effect of a rolling rotation of the wing), or variations such as $\alpha(y) = H(s, y)\alpha_T - H(s, -y)\alpha_T$, which corresponds to antisymmetrically deflected ailerons. Consider such a wing with the symmetric chord variation [Eq. (23a)] and an antisymmetric variation of incidence defined by

$$\bar{\alpha}(y) = \sum_{j=0}^{2n+1} \left[S_{\text{gn}}(y)\bar{\alpha}_j + H(s, y)\bar{\alpha}_j^* - H(s, -y)\bar{\alpha}_j^* \right] |y|^j \qquad (26)$$

where $H(s, y)$ and $H(s, -y)$ are defined in the Nomeclature and $S_{\text{gn}}(y)$ represents the sign of y, that is, $S_{\text{gn}}(y) = 1$ for $y > 0$ and $S_{\text{gn}}(y) = -1$ for $y < 0$. In this case [$\beta_k^S = 0$, $\beta_k^A = \beta_k$, and $\hat{\beta}_k^1 = (-1)^{k+1}\hat{\beta}_k^2 = \hat{\beta}_k$], the general solution (12) of the circulation is simplified as

$$\bar{\Gamma}(y) = \sum_{k=0}^{2n} \beta_k F_k^1(y) + \sum_{k=0}^{\hat{n}} \hat{\beta}_k [\hat{F}_k(s, y) - \hat{F}_k(s, -y)] \qquad (27)$$

The new functions $\hat{F}_k(s, y) - \hat{F}_k(s, -y)$ represent the specific contributions of the antisymmetric changes of the wing incidence at $y = s$ and $y = -s$.

The unknown coefficients β_k can be determined from the following system of equations:

$$\{\tilde{B}_{i,k} + \breve{B}_{i,k}\}[\beta_k] + \left\{\tilde{B}_{i,k}^*\right\}[\hat{\beta}_k] = \left[D_i + D_i^*\right] \qquad (28a)$$

$$\tilde{B}_{i,k} = E_{i,k} + \frac{\pi}{k+1} \sum_{j=0}^{k} \ell_{j+1} I_{k-j} P_{j+i} + g_{k,0} \frac{I_{k+i+1}}{k+i+2} \qquad (28b)$$

$$\tilde{B}_{i,k}^* = E_{i,k}^* + \frac{\pi}{k+1} \sum_{j=0}^{k} \ell_{j+1} J_{k-j}(s) P_{j+i} - 2g_{i,0} \frac{s^{k+i+2}}{k+i+2} G_0(s) + \frac{\sqrt{1-s^2}}{k+i+2} \left\{ \frac{2}{k+1} \sum_{j=0}^{k} \ell_j I_{j+i+1} s^{k-j} - \sum_{j=0}^{i} g_{i,j+1} I_j s^{k+1+i-j} \right\} \qquad (28c)$$

where D_i, $E_{i,k}$, $\breve{B}_{i,k}$, D_i^*, $E_{i,k}^*$, and $g_{i,j}$ are defined in Eqs. (20) and (25) and in the Nomenclature.

2. Trapezoidal and Rectangular Wings with Antisymmetric Incidence Changes

The solution (27) of the circulation is shown in Fig. 8 for the following cases of rectangular ($q = 0$) and trapezoidal ($q = 0.6$) wings with $\lambda = 9$: 1) wings with a continuous antisymmetric linear variation of incidence $\alpha(y) = \alpha_T y$ (which may correspond to the effect of a rolling rotation of the wing); and 2) wings with sudden antisymmetric changes of incidence, from $\alpha_R = 0$ to $\pm\alpha_T$, at $y = \pm s$, for $s = 0.4$, 0.5, and 0.6 (which may correspond to the effect of antisymmetrically deflected ailerons located on the wing). The nondimensional circulation $\bar{\Gamma}_T(y) = \Gamma(y)/[2b\alpha_T U_\infty]$ is used in this case.

In all of these cases, the present solutions are found to be in good agreement with the panel method (Katz and Plotkin[6]) results.

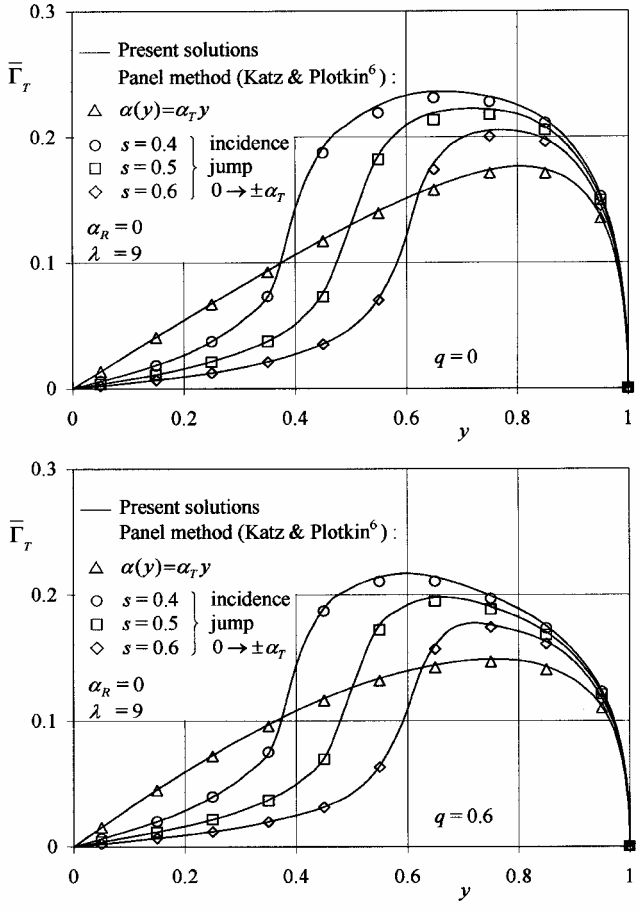

Fig. 8 Wings with antisymmetric incidence variation. Distribution of $\bar{\Gamma}_T(y) = \Gamma(y)/[2b\alpha_T U_\infty]$ along span for 1) linear incidence variation $\alpha(y) = \alpha_T y$ and 2) incidence changes caused by antisymmetric deflections of ailerons at three locations $y = \pm s$.

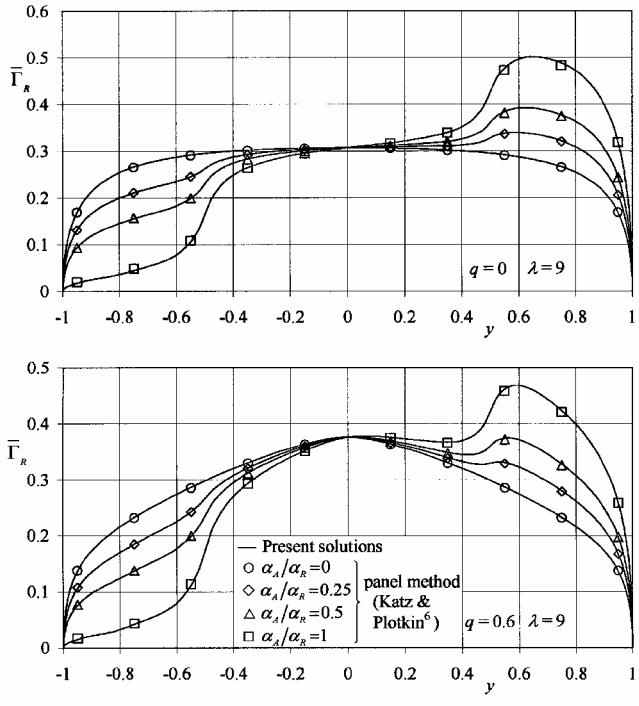

Fig. 9 Wings with asymmetric incidence variation caused by antisymmetric aileron deflections: variation of $\bar{\Gamma}_R(y)=\Gamma(y)/[2b\alpha_R U_\infty]$ along span.

This further confirms the utility of the functions $\hat{F}_k(s, y) - \hat{F}_k(s, -y)$, representing the specific contributions of the antisymmetric changes of the wing incidence at $y = s$ and $y = -s$.

B. Wings with Asymmetric Incidence Variation

In many flight conditions asymmetric incidence variations can occur as a result of the combined effects of the wing incidence, symmetrically deflected flaps, and antisymmetrically deflected ailerons. In this case the wing circulation distribution is given by the general solution (12), or, alternatively, it can be obtained by a convenient summation of the symmetric and antisymmetric solutions (19), (24), and (27).

The solutions for wings with asymmetric incidence distribution, generated by a symmetric wing incidence and antisymmetrically deflected ailerons, are illustrated in Fig. 9 for rectangular ($q = 0$) and trapezoidal ($q = 0.6$) wings of aspect ratio $\lambda = 9$ with the incidence distribution

$$\alpha(y) = \alpha_R + H(s, y)\alpha_A - H(s, -y)\alpha_A \qquad (29)$$

where $s = 0.5$. The nondimensional circulation $\bar{\Gamma}_R(y) = \Gamma(y)/[2b\alpha_R U_\infty]$ is used in this figure to compare the influence of the antisymmetric incidence changes $\alpha_A/\alpha_R = 0$, 0.25, 0.5, and 1. One can notice that all circulation distributions for the trapezoidal wings have a slope discontinuity at $y = 0$, in contrast to the rectangular wings; this confirms the importance of the forced symmetry and antisymmetry terms that are taken here into account for the first time in this work.

The present solutions were found in good agreement, in all cases, with the panel method (Katz and Plotkin[6]) results.

VI. Conclusions

A new method of solution has been presented for the incompressible flow over finite-span wings of arbitrary shapes. This new method avoids the difficulties of the previous methods. Velocity singularities placed in the Trefftz plane are used to derive the contributions of the changes in the wing chord and incidence variations along span to the solution of the spanwise distribution of the circulation.

New functions are derived for these contributions to provide a correct mathematical modeling of the physical wing, and they contain both natural and forced symmetry and antisymmetry terms. Because of the forced terms, the circulation distribution of trapezoidal wings has a discontinuous slope at the root chord, in contrast to that of rectangular wings. The new forced symmetry and antisymmetry terms and the new contributions of the changes in the incidence and chord variations are absent in the previous methods. Thus in the new method the solution has a high level of accuracy and is free of spurious spanwise oscillations.

This new method is successfully validated by comparison with the solutions obtained by Rasmussen and Smith[22] and Carafoli[4] for the rectangular and tapered wings of uniform incidence and with the results of a panel method (Katz and Plotkin[6]). The method is then used to obtain solutions of aeronautical interest for wings with symmetric and antisymmetric incidence variations that might arise as result of the deflections of the control surfaces, such as flaps and ailerons. Solutions are also easily obtained for wings with curved leading and trailing edges and variable incidence; the curved edges of such wings are difficult to model in panel methods.

The new method provides very efficient, robust, and accurate theoretical solutions in all cases studied, including the asymmetric incidence variations that can occur in various flight conditions.

Acknowledgments

The support of the Natural Sciences and Engineering Council of Canada is gratefully acknowledged, as well as the contributions to the initial calculations made by the former graduate students A. Dziubinschi and G. Dziubinschi.

References

[1]Glauert, H., *The Elements of Aerofoil and Airscrew Theory*, 2nd ed., Cambridge Univ. Press, Cambridge, England, U.K., 1959, Chap. 10, 11.

[2]Anderson, J. D., *Fundamentals of Aerodynamics*, 2nd ed., McGraw–Hill, New York, 1991, Chap. 5.

[3]Bisplinghoff, R. I., Ashley, H., and Halfman, R. L., *Aeroelasticity*, Addison Wesley Longman, Reading, MA, 1955, pp. 229–238.

[4]Carafoli, E., *Tragflügeltheorie*, VebVerlag, Berlin, 1954, Chap. 15–18.

[5]Karamcheti, K., *Ideal-Fluid Aerodynamics*, Wiley, New York, 1966, Chap. 19.

[6]Katz, J., and Plotkin, A., *Low-Speed Aerodynamics*, McGraw–Hill, New York, 1991, Chap. 8.

[7]Katz, J., "Calculation of the Aerodynamic Forces on Automotive Lifting Surfaces," *Journal of Fluids Engineering*, Vol. 107, No. 12, 1985, pp. 438–443.

[8]Kuethe, A. M., and Chow, C.-Y., *Foundations of Aerodynamics*, Wiley, New York, 1986, Chap. 6.

[9]Milne-Thomson, L. M., *Theoretical Aerodynamics*, Dover, New York, 1966, Chap. 11.

[10]McCormick, B. W., *Aerodynamics, Aeronautics and Flight Mechanics*, Wiley, New York, 1995, Chap. 3, 4.

[11]Robinson, A., and Laurmann, J. A., *Wing Theory*, Cambridge Univ. Press, Cambridge, England, U.K., 1956, Chap. 3.

[12]Schlichting, H., and Truckenbrodt, E., *Aerodynamics of the Airplane*, McGraw–Hill, New York, 1979, Chap. 3.

[13]Thwaites, B., *Incompressible Aerodynamics*, Oxford Univ. Press, Oxford, England, U.K., 1960, Chap. 8.

[14]Von Mises, R., *Theory of Flight*, Dover, New York, 1959, Chap. 3.

[15]Multhopp, H., "The Calculation of the Lift Distribution of Airfoils," British Ministry of Aircraft Production, R. T. P. 2392, (from *Luftfahrtforschung*), Bd. 15, No. 14, 1938, pp. 153–169.

[16]Bertin, J. A., and Smith, M. L., *Aerodynamics for Engineers*, 3rd ed., Prentice–Hall, Upper Saddle River, NJ, 1998, Chap. 7.

[17]Anderson, R. C., and Millsaps, K., "Application of the Galerkin Method to the Prandtl Lifting-Line Equation," *Journal of Aircraft*, Vol. 1, No. 3, 1964, pp. 126–128.

[18]Bera, R. J., "Some Remarks on the Solution of the Lifting-Line Equation," *Journal of Aircraft*, Vol. 11, No. 10, 1974, pp. 647, 648.

[19]Berbente, C., "On a Method for the Aerodynamic Calculation of Finite-Span Wings in Incompressible Flow," *Buletinul Institutului Politehnic Bucuresti*, Vol. 35, No. 5, 1973, pp. 1–13.

[20]Carafoli, E., *Aérodynamique des Ailes d'Avions*, Chiron, Paris, 1928.

[21]Lotz, I., "Berechnung der Auftriebsverteilug Beliebig Geformter Flugel," *Zeitschrift für Flügtechnik und Motorluftschiffahrt*, Vol. 22, No. 7, 1931, pp. 189–195.

[22]Rasmussen, M. L., and Smith, D. E., "Lifting-Line Theory for Arbitrarily Shaped Wings," *Journal of Aircraft*, Vol. 36, No. 2, 1999, pp. 340–348.

[23]Mateescu, D., and Newman, B. G., "Analysis of Flexible-Membrane and Jet-Flapped Airfoils Using Velocity Singularities," *Journal of Aircraft*, Vol. 28, No. 11, 1991, pp. 789–795.

[24]Mateescu, D., "Wing and Conical Body of Arbitrary Cross-Section in Supersonic Flow," *Journal of Aircraft*, Vol. 24, No. 4, 1987, pp. 239–247.

[25]Mateescu, D., "A Hybrid Panel Method for Aerofoil Aerodynamics," *Boundary Element XII*, Vol. 2, Springer-Verlag, Berlin and New York, 1990, pp. 3–14.

[26]Mateescu, D., and Nadeau, Y., "A Nonlinear Analytical Solution for Airfoils in Irrotational Flows," *Proceedings of the 3rd International Congress of Fluid Mechanics*, edited by A. H. Nayfeh, Vol. 4, Cairo, 1990, pp. 1421–1423.

[27]Mateescu, D., "Steady and Unsteady Flow Solutions Using Velocity Singularities for Fixed and Oscillating Airfoils and Wings," *Computational Methods and Experimental Measurements X*, Computational Mechanics Publications, Southampton and Boston, 2001, pp. 3–12.

[28]Mateescu, D., and Abdo, M., "Theoretical Solutions for Unsteady Flows Past Oscillating Flexible Airfoils Using Velocity Singularities," *Journal of Aircraft*, Vol. 40, No. 1, 2003, pp. 153–163.

[29]Carafoli, E., Mateescu, D., and Nastase, A., *Wing Theory in Supersonic Flow*, Pergamon Press, Oxford, England, U.K., and New York, 1969, Chap. 2.